J. Membrane Biol. 129, 81–97 (1992)

The Journal of
Membrane Biology

Whole-Cell Potassium Current in Rabbit Corneal Epithelium Activated by Fenamates

James L. Rae†§ and Gianrico Farrugia†‡
Departments of †Physiology and Biophysics, ‡Gastroenterology, and §Ophthalmology, Mayo Foundation, Rochester, Minnesota 55905

Summary. Rabbit corneal epithelium contains a large-conductance, potassium-selective channel, which is a major contributor to the whole-cell current. In perforated-patch recordings of the macroscopic current, the isolated cells studied had resting voltages of -41 ± 20 mV and capacitances of 5.8 ± 2.6 pF (mean ± SD for $n = 255$). Activation of the channels was weakly voltage dependent. They opened at about -100 mV and reached an open probability of about 0.2 at $+100$ mV. The current was blocked by millimolar concentrations of external Ba^{2+} and quinidine. Diltiazem also blocked when applied to the external surface of the membrane. Nonsteroidal anti-inflammatory agents of the fenamate group were powerful activators of the channel at submillimolar concentrations when applied either to the inside or the outside of the channels. The mechanism of action which leads to his activation is not yet known.

Key Words cornea · epithelium · patch clamp · potassium current · fenamates

Introduction

The corneal epithelium by virtue of its ubiquitous tight junctions provides a barrier to penetration of many water-soluble substances (Wolosin, 1988). In addition, it is known to transport a small amount of fluid from its stromal side to its tear side (Klyce, 1975; Marshall & Klyce, 1984; Klyce & Crosson, 1985; Reinach, 1985). To produce that fluid transport, there is a bumetanide- and furosemide-sensitive NaCl cotransport system located on the basolateral side of the corneal epithelium (Candia & Schoen, 1978; Candia, Grillone & Chu, 1986; Nagel & Carrasquer, 1989). This serves as a Cl-entry step to raise internal Cl above electrochemical equilibrium. On the tear or apical side of the corneal epithelium, there exist Cl-conductive channels which, when open, allow downhill movement of Cl into the tears (Marshall & Hanrahan, 1991). This mechanism is quite similar to that found in other Cl-secreting epithelia, and much of the early investigation of Cl transport was done using corneal epithelium. The energy for the Cl entry comes from the Na gradient which inevitably depends upon the function of the Na-K ATPase in the cells. While K channels are not *directly* involved in this fluid transport scheme, the Na pump which is involved requires a K channel to provide the backflux of K to balance the pump current (Reinach, Candia & Alvarez, 1979; Candia & Cook, 1986). In addition, K channels are involved in volume regulation in many cells and are often the dominate contributors to the resting conductance of cells and thus to their resting voltage. It is, therefore, important to understand the function and properties of these vital transporters.

The basolateral cells of the bullfrog and rabbit corneal epithelium are known to be dominated by K conductances (Akaike & Hori, 1970; Akaike, 1971; Reinach & Nagel, 1984, 1985; Clausen, Reinach & Marcus, 1986; Reinach, Thurman & Klemperer, 1987; Wolosin & Candia, 1987*a*; Reinach & Schoen, 1990). Recent experiments (Wolosin & Candia, 1987*a*) have suggested that in both species there are at least two different K conductances, one a resting background conductance and the other a conductance stimulated by cell swelling. Several investigators have found that the resting basolateral K conductance is blocked by millimolar concentrations of Ba applied to the bathing solution (Reinach & Nagel, 1984). Wolosin and Candia (1987*b*) showed that their volume-activated current could be blocked by *both* barium and quinidine. Interestingly, Reinach (1985) and Huff and Reinach (1985) showed that the basolateral K conductance in isolated bullfrog cornea epithelium could be blocked by diltiazem, a compound most often used at lower concentrations to block Ca channels.

Using patch-clamp techniques, we have recently characterized the properties of a large-conductance, K-selective channel from rabbit corneal epithelium which is likely responsible for at least part of the macroscopic conductances previously

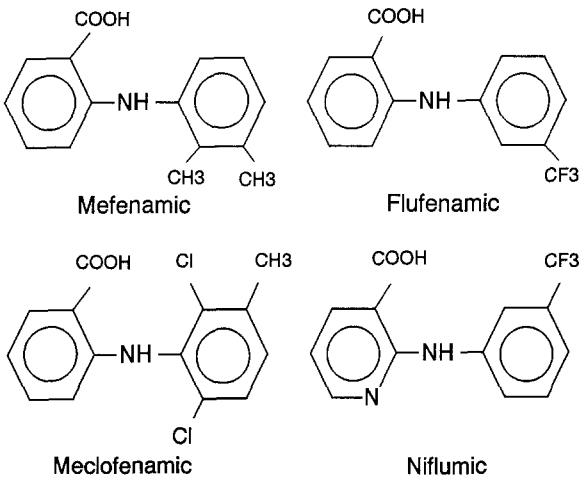

Fig. 1. Structures of the four fenamates used.

reported (Keys et al., 1986; Rae, Levis & Eisenberg, 1988; Rae, et al., 1990). This K channel has a conductance of about 170 pS in symmetrical 150 mM K solutions, shows weak voltage dependence to its activation, and is not saturated at any physiologically realizable K concentration. It is also stretch activated and blocked by cesium, barium, and quinidine (Rae, Dewey & Rae, 1992) applied to the external bathing solution.

In the studies reported here, we use fenamates (Wangemann et al., 1986), nonsteroidal anti-inflammatory agents, which are used therapeutically primarily because of their inhibitory effect on the cyclo-oxygenase pathway (Terada, Muraoka & Fujita, 1974). These compounds (Fig. 1), which include mefenamic, flufenamic, meclofenamic, and niflumic acids, have been shown to have an effect on membrane-transport proteins in several systems. For example, flufenamic acid interferes with the action of band three protein and thus anion transport in erythrocytes (Knauf & Mann, 1984). White and Aylwin (1990) found it to be an inhibitor of Ca-activated Cl channels in *Xenopus* oocytes, whereas Gogelein and coworkers (1989, 1990) found fenamates to be potent blockers of nonselective-cation channels when applied to their cytoplasmic side. We find that these compounds are also potent *activators* of a K current in rabbit corneal epithelium.

In this manuscript, we quantify whole-cell currents obtained by perforated-patch recording techniques applied to freshly dissociated rabbit corneal epithelial cells. We also show that the majority of the whole-cell current comes from the large-conductance K channel, that the channel is open at the resting voltage, and that it is stimulated by fenamates and blocked by external diltiazem.

Materials and Methods

All experiments were done on New Zealand white rabbits with an average weight between 2.5 and 3 kg. The animals were treated in accordance with the Association for Research in Vision and Ophthalmology (ARVO) guidelines for the use of experimental animals in eye research. The animals were sacrificed by an overdose of sodium pentobarbital injected into a marginal ear vein.

Following removal of the globe, the corneas were dissected free via a 360° incision at the limbus. In general, the endothelium and Descemet's membrane were removed for other experiments and the remaining stroma and corneal epithelium were placed in a petri dish in an enzyme-based dissociation fluid (Table) and incubated at 37°C for 70–90 min in a 95% oxygen, 5% CO_2 environment. The epithelial cells were then triturated from the corneal stroma using a Pasteur pipette. The trituration fluid and suspended cells were placed in a 15-ml centrifuge tube, and the cells spun down at about 180 × *g*. The cells were then resuspended in a NaCl-based Ringer containing glucose.

Recording Techniques

Approximately 100 μl of the cell suspension were placed in a Ringer-filled well in an acrylic plastic chamber located under a compound microscope. The chamber bottom was lined with a small piece of microscope slide glass cleaned with ethanol. The cells eventually settled to the bottom of the chamber where they attached to the glass substrate. The patch-clamp recordings were made using either Corning #7760 or Kimble KG-12 glass electrodes pulled on a Sutter Instruments (Novato, CA) Model P-80 microelectrode puller. The tips were coated with Dow Corning (Midland, MI) Slygard® #184 to within 100 μm of the tip and then fire polished under direct observation at 1500-diameter magnification. The majority of the results reported here were obtained using a perforated-patch technique with amphotericin B (Sigma #A-4888) as the perforating agent. For this procedure, electrode tips were filled by dipping into an amphotericin-free filling solution and then backfilling the electrode with the same solution containing 120–240 μg/ml of amphotericin B. The electrodes were mounted in a polycarbonate holder of an Axopatch 200 or 1B (Axon Instruments, Foster City, CA) patch voltage clamp and pressed against the membranes of desired cells under direct observation. Following the application of suction, gigohm seals were routinely obtained. Within 5 to 10 min, the amphotericin partitioned into the membrane patch isolated in the pipette tip and routinely produced access resistances between 5 and 20 MΩ to allow voltage clamping of the cells. The Axopatch 200 or 1B were connected to a TL-1 Labmaster interface (Axon Instruments) driven by PClamp software (Axon Instruments) to allow the delivery of quite complicated voltage-step protocols with concomitant digitization of the current. In general, the digitization rate was 2 kHz for currents filtered at 1 kHz through an 8-pole Bessel filter. In most experiments, the voltage-step protocols were repeated at least five times and the resultant currents at each voltage averaged to produce the final records.

The subsequent analyses of the current were done using either Clampfit, a program supplied with PClamp, or using custom macros in Excel (Microsoft, Redmond, WA). Final plots were done using Excel, PaintBrush 4 (ZSoft, Atlanta, GA) and Sigma Plot (Jandel, Madera, CA).

Table. Solutions

Solution	Na	K	Cl	Me	Ca	Glucose	HEPES	EGTA	Trypsin
Normal Ringer	146	4.7	154.7	0	2	5	5	0	0
KCl Ringer	0	150	154	0	2	5	5	0	0
K110/Na40	40	110	154	0	2	5	5	0	0
K75/Na75	75	75	154	0	2	5	5	0	0
K40/Na110	110	40	154	0	2	5	5	0	0
K20/Na130	130	20	154	0	2	5	5	0	0
Pipette-filling	0	150	25	125	0	0	5	2	0
Dissociation	149.2	4.7	153.9	0	0	0	5	0	0.001%

All values are in millimolar; pH = 7.3–7.4; osmolality ≈ 300 mOsm.

Solutions

The solutions used in the experiments are shown in the Table.

Drugs

Mefenamic, flufenamic, niflumic and meclofenamic acids as well as quinidine and diltiazem were obtained from Sigma Chemical (St. Louis, MO).

Corrections for Junction Potentials and Series Resistance

For the pipette-filling solutions utilized for these studies, the liquid junction potential calculated from the Henderson equation (Lewis & Sargent, 1909) is between 8 and 10 mV. We tested for the need to correct for a junction potential of this magnitude experimentally by measuring the K current from single cells when the pipette and bathing solution contained symmetrical solutions. Under these circumstances, the K current must reverse at 0 mV. In most cases, we found a reversal potential between +8 and +13 mV which should be the combination of the liquid junction potential and the Donnan potential produced by mismatch of pipette and cellular anions. Therefore, for all current-voltage relationships determined, the voltage axis was corrected by subtracting 10 mV from each voltage.

Series-resistance correction was done off-line rather than using the circuitry in the patch clamp since we did not require series-resistance compensation to increase the recording bandwidth. Since the 10 to 90% rise time for the current (R_T) was about 90 msec, the bandwidth ($BW \approx R_T/0.35$) is ≈26 Hz. The bandwidth limit for the recordings is approximated by

$$BW = \frac{1}{2\pi R_a C_m} \quad (1)$$

where R_a = access resistance and C_m = membrane capacitance. Since the average capacitance of our cells was approximately 6 pF, even for an R_a as high as 100 MΩ, the bandwidth of the recording would be approximately 300 Hz or 10 times the bandwidth of the current itself. With R_a's < 20 MΩ, typical for these experiments, $BW > 1500$ Hz. We, therefore, needed no correction for dynamic response and so corrected for series resistance by simply subtracting the current-resistance (IR) drop across the pipette tip from the pipette voltage itself and replotted the data using this corrected voltage on the x-axis.

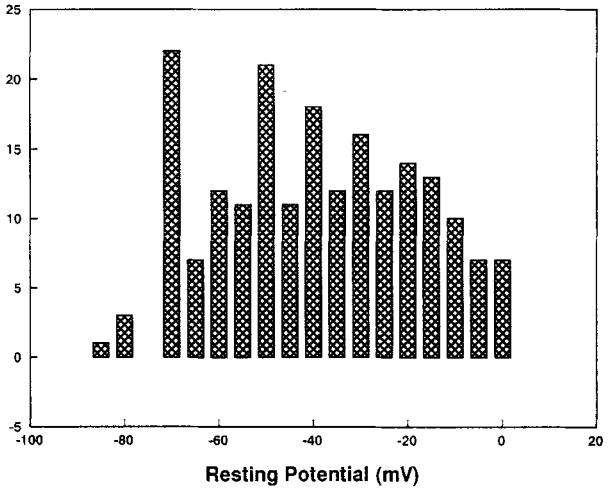

Fig. 2. Histogram of the resting voltages for the cells used in this study. Resting voltages were determined either from the reversal potential of the macroscopic current in voltage clamp and/or from the command voltage required to make the steady-state current zero in current clamp. The histogram was constructed using a transform in Sigmaplot.

Results

Cell Morphology, Resting Potentials and Membrane Capacitance

The dissociated cells come from all layers of the corneal epithelium, and no attempt was made to physically separate different types. The cells from near the surface are flat and much larger than the deeper cells. These surface cells were not used for these studies. The cells utilized (N = 255) had capacitances of 5.8 ± 2.6 pF and average resting potentials of −40.7 ± 20.4 mV. A histogram of the resting potentials determined from the reversal potential of the macroscopic current is given in Fig. 2. The cells

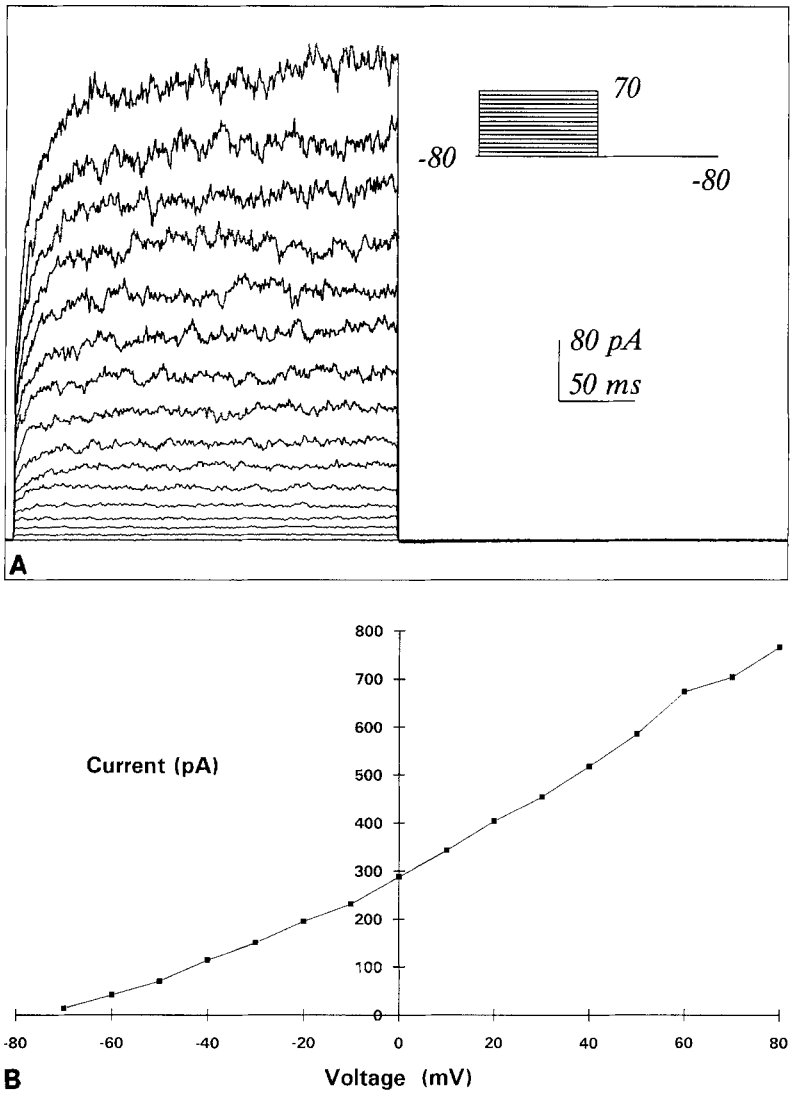

Fig. 3. (*A*) Whole-cell current records from a single corneal epithelial cell voltage clamped through an amphotericin-B-perforated patch.The records were filtered through a 1-kHz 8-pole Bessel filter and sampled at 2 kHz. The voltage protocol used is shown in the figure. (*B*) Steady-state *I-V* determined for one of the cells with a substantially negative resting potential. Reversal of the current occurs beyond −75 mV.

had resting voltages which ranged from a high of −85 to a low of 0 mV. All the cells but three contained the K current, which we report here, but the cells with lower resting voltages contained larger leak conductances than did the cells with higher resting voltages.

Form of the Whole-Cell Current

Figure 3*A* shows a perforated-patch whole-cell recording from a typical corneal epithelial cell. The transmembrane voltage was held at −80 mV and then stepped to a series of more depolarized voltages in 10-mV steps, returning to −80 mV following each step. Even after five averages, the currents are quite noisy due to the fact that they are largely derived from a K channel with a large single-channel conductance. There is a jump in the current instantly following the onset of the voltage step, and then the current increases over the next 50 to 100 msec. This jump, which was present even in cells with extremely low leak conductances, suggests that some fraction of the channels are open at the holding voltage of −80 mV.

A typical steady-state current-voltage relationship is plotted in Fig. 3*B*. These particular data are taken from a cell with a small leak conductance and a resting potential of about −75 mV as shown from the zero current potential of the *I-V*. The current is increasingly activated with depolarization but shows no evidence of saturation over a voltage range of −70 to +80 mV. The steady-state *I-V* also shows that the current is highly K selective. For the internal and external solutions used, $E_K \approx -87$ mV and $E_{Cl} \approx -45$ mV. Since the current is outward by −70 mV, it must be carried largely by K. Substitution of methanesulfonate for Cl in the bath also had no effect

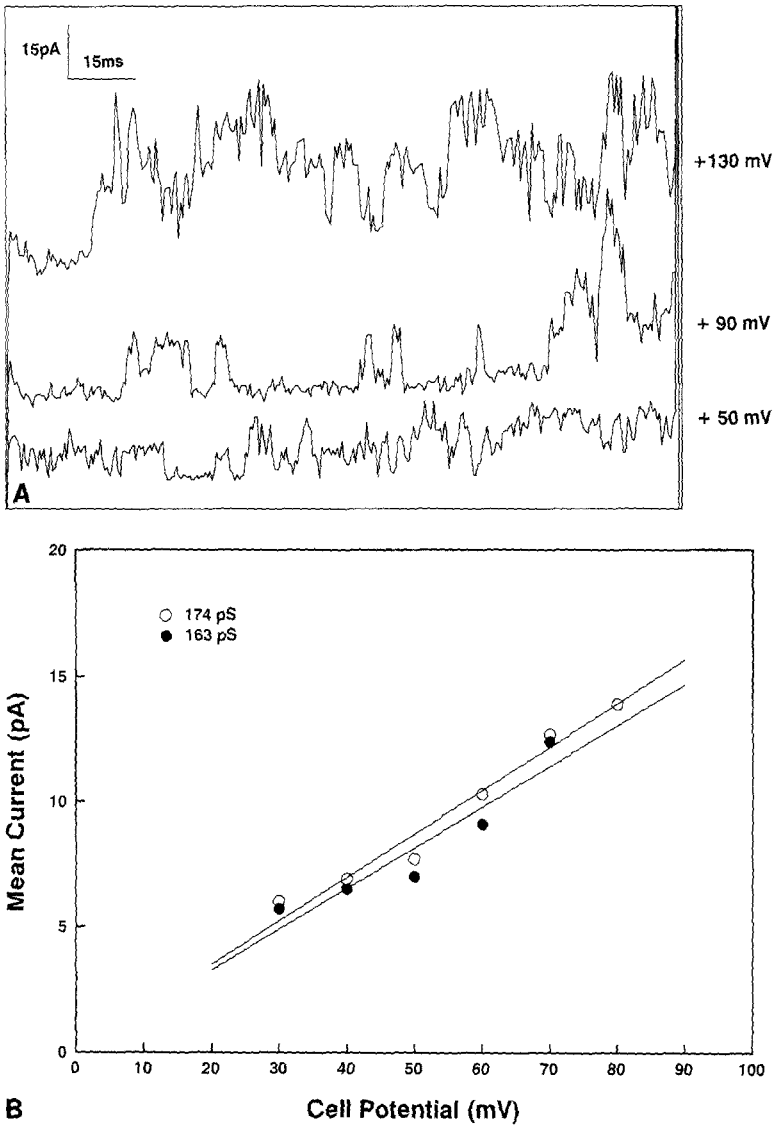

Fig. 4. (*A*) Three unaveraged current sweeps following voltage steps from −80 to +50, +90, and +130 mV to show the noisy nature of the current. *BW* = 1kHz (8-pole Bessel filter). (*B*) Current-voltage relationships from single current sweeps following voltage steps to several voltages in two cells whose total current was sufficiently small that single-channel gating transitions could be discerned in the whole-cell records.

on the reversal potential of the current if, of course, corrections were made for junction potentials. Throughout these experiments, it proved reasonable to model the currents as coming from K channels (I_K) in parallel with a leak current (I_{leak}). We define a leak current as one with an ohmic *I-V* and reversal potential of 0 mV.

Figure 4*A* displays the current elicited by single voltage steps from −80 to +50, +90 and +130 mV. The extremely noisy nature of the unaveraged current is apparent. When data of this kind were displayed on a faster time scale, it was possible to identify discrete steps in the whole-cell current which were related to the gating of single channels. Current-voltage relationships constructed from two such experiments are shown in Fig. 4*B*. The solid lines are simple linear regressions through the data points. The apparent single-channel conductance at substantial depolarizing voltages where the single-channel currents could be measured was 163 pS in one cell and 174 pS in the second. These numbers compare well with the 167 pS measured previously in single-channel experiments with the channel bathed in symmetrical 150 mM K solutions. These results make it likely that the single-channel currents that we have previously characterized contribute substantially to the macroscopic whole-cell currents measured here.

Probability of Opening

The channels are open at the resting voltage of the cell, a necessary result if this current is to be a major contributor in the control of the resting voltage of

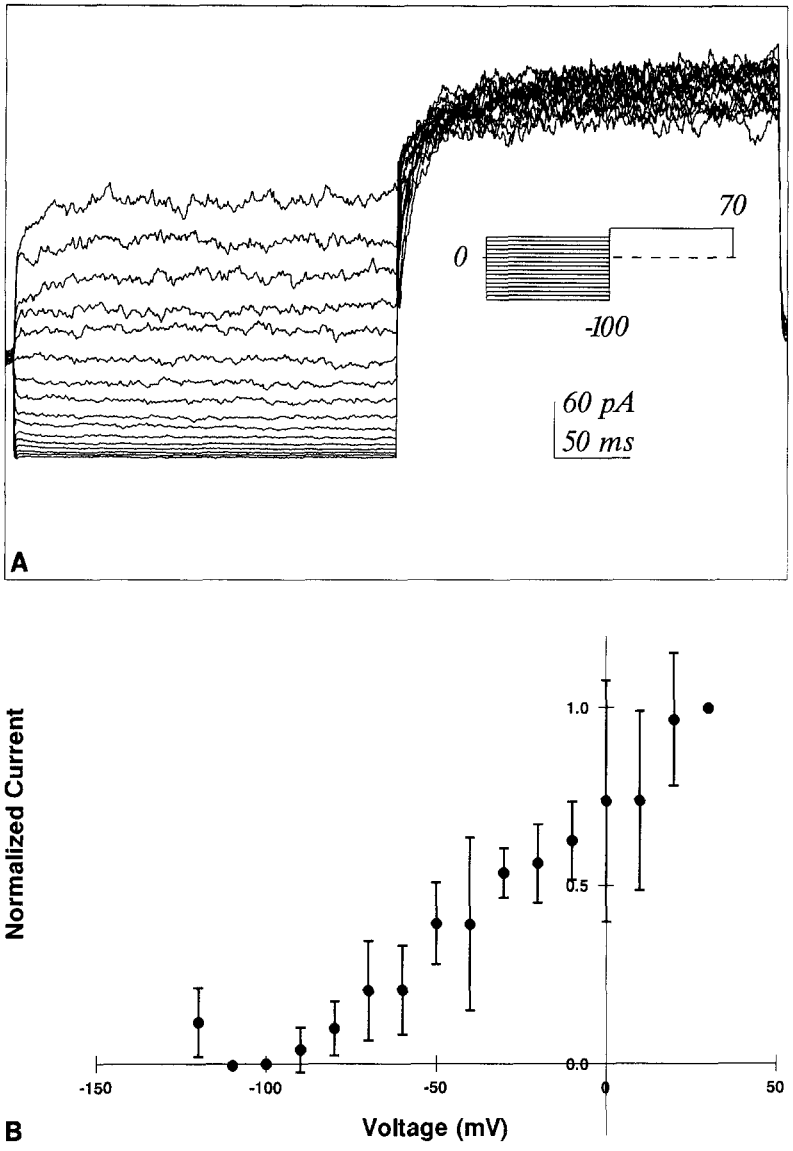

Fig. 5. (*A*) Current records from a perforated-patch whole-cell recording obtained using the voltage-step protocol shown. BW = 1 kHz (8-pole Bessel filter). (*B*) Overplot of the instantaneous current-voltage relationships obtained from three cells subjected to the protocol in *A*. The current is that immediately following the step to +70 mV, and the voltages are those just preceding the steps to +70 mV. The currents are normalized to be ≈1.0 at +30 mV and ≈0 at −100 mV. The values are the mean ± SD from three cells.

the cell. To demonstrate this, the cells were held at 0 mV and stepped to a series of both hyperpolarized and depolarized activating voltages. The current was allowed to reach steady state (Fig. 5*A*). The voltage was then stepped to +70 mV. The instantaneous current measured immediately following the step to +70 mV will contain the current flowing through the leak conductance and the currents flowing through the channels which were open at the previous activating voltage. Assuming that the leak current at this single voltage does not depend upon the activating voltage, any change in the instantaneous "tail currents" at different activating potentials should be due to changes in currents flowing through open channels. Figure 5*B* shows data collected from three cells using this protocol. The current is normalized so that its value at +30 mV is 1 and its value at −100 mV is 0. All three records show clearly that the channels begin to open at a voltage of about −100 mV, clearly more hyperpolarized than the physiological (≈ −60 mV) resting voltage of these cells (Akaike & Hori, 1970; Ehlers, 1970; Fee & Edelhauser, 1970; Klyce, 1972, 1973; Wiederholt & Koch, 1978; Reuss et al., 1983).

The increase in current with depolarization shows weak dependence on voltage. This was quantified by measuring the instantaneous tail current generated at a fixed voltage of −80 mV following activation of the current by a series of depolarizing voltage steps. A current-voltage relationship constructed from these instantaneous tail currents plotted against the activating voltage just prior to generation of the tail currents is shown in Fig. 6. This curve, which presumably measures the inward cur-

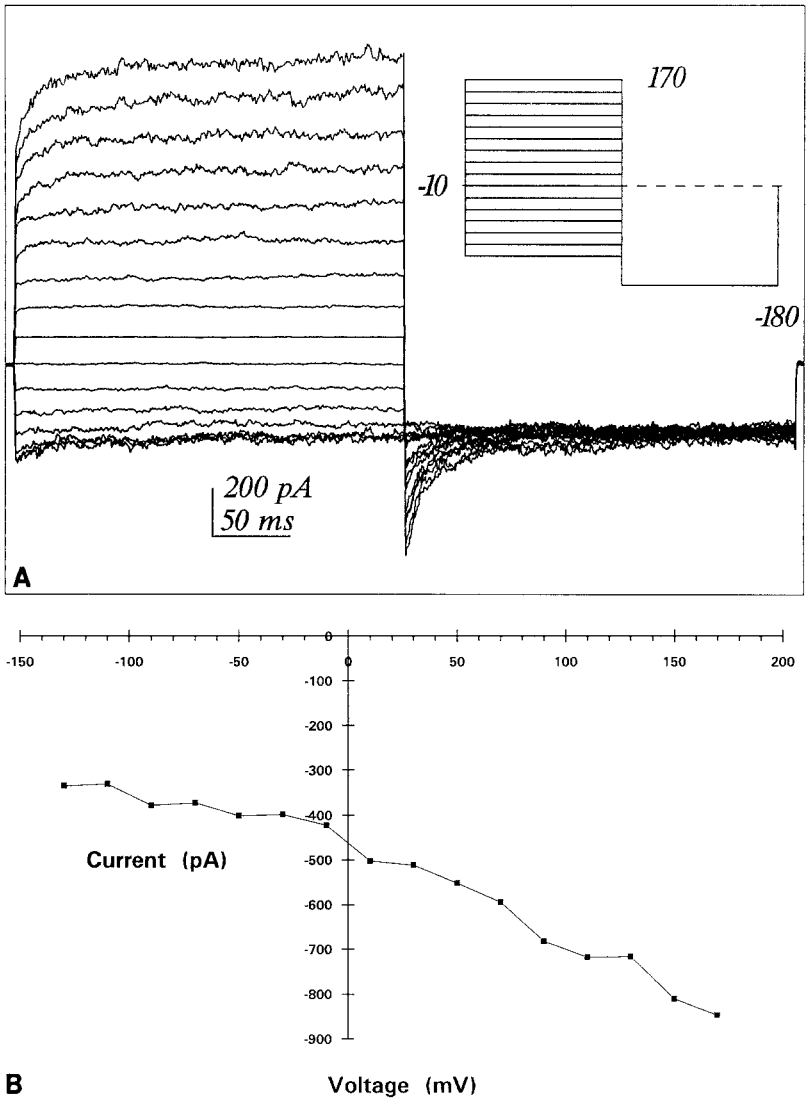

Fig. 6. (*A*) Whole-cell currents from a typical cell bathed in 150 mM KCl obtained using the voltage protocol shown in the figure. (*B*) Tail currents generated from the cell in *A* bathed in 150 mM KCl Ringer (Table). The cell, whose resting voltage was 0 mV in these solutions, was held at −80 mV, stepped for 250 msec to the voltages shown on the voltage axis and then returned to −80 mV. The current plotted is that obtained immediately upon returning to −80 mV.

rent through channels opened at the previous activating voltages, should have the same shape as the open probability *versus* voltage curve. Tail currents generated in this way show that the channel is open at the resting voltage but does not achieve a unit open probability even by +180 mV.

Selectivity

The selectivity of the current can be shown easily using a tail current protocol in which the cells are held at −80 mV, stepped to +70 mV to activate the channels, and then stepped to a series of voltages between −115 and +35 in 15-mV steps. This protocol is repeated on the same cell with different Na and K mixtures in the bathing solution. The reversal potential of the instantaneous tail currents should be very near E_K for a K-selective current. Because many of our cells also contained a leak conductance, we sometimes used a more extensive protocol to extract the K-selective currents. We first generated currents according to the above protocol except that the activating voltage was −100 mV where most of the channels are closed instead of +70 mV where many of the channels are open. By using the difference in instantaneous tail currents between those generated at an activating voltage of +70 mV and those at an activating voltage of −100 mV, we were able to subtract off the majority of the leak conductance and determine more specifically the tail currents that depended on the activating voltage. A representative result is shown in Fig. 7. Clearly, the reversal potential becomes more and more negative as the external K concentration is reduced and the inward conductance falls as the external K concentration falls. The reversal potentials are very near

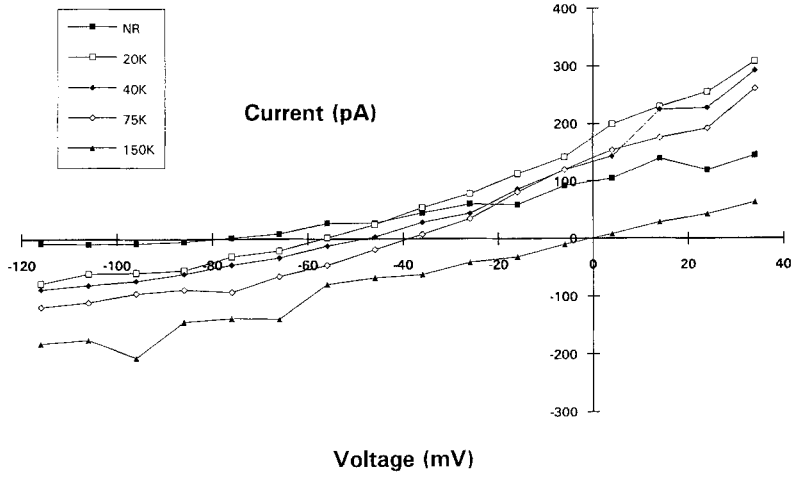

Fig. 7. Instantaneous current-voltage relationships determined from the difference in a family of tail currents generated following an activation voltage to first −100 mV and then +70 mV (*see* text).

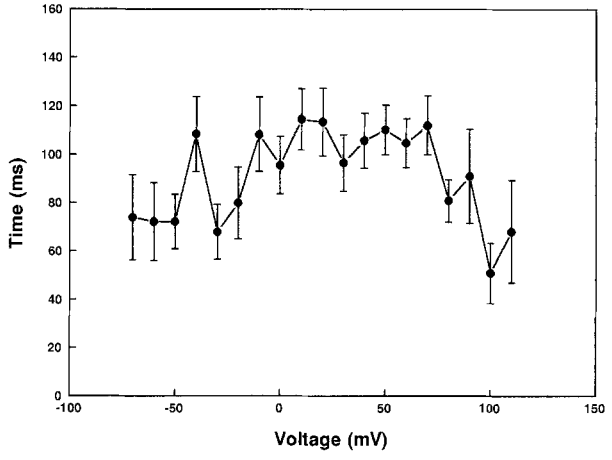

Fig. 8. Plots of the 10–90% rise time for the whole-cell current following voltage steps from −80 mV to the voltages plotted on the x-axis. Values are mean ± SE for $n = 19$. The rise time shows little dependence on voltage.

those expected for a perfectly K-selective channel. From a model where

$$I_{\text{total}} = I_{\text{leak}} + I_{\text{K}} = 0$$

and

$$I_{\text{K}} = g_{\text{K}}(E_m - E_{\text{K}})$$

and

$$I_{\text{leak}} = g_L E_m, \quad \frac{E_m}{E_{\text{K}}} = \frac{g_{\text{K}}}{g_{\text{K}} + g_L}. \tag{2}$$

Here g_{K} and g_L are the macroscopic conductances for K and the leak, respectively, and all other variables have their usual meaning. From the ratio of E_m/E_{K} in Fig. 7, $g_{\text{K}} \approx 95\%$ of the total conductance in the model and so the current is highly selective for K by this measure. Whether the "leak" comes from Na permeation through the same channel or from a separation leak pathway not removed by our protocol cannot be determined at present.

Activation Kinetics

Kinetically, the currents are not very complex. The activation time course of the channels following steps from −80 mV to depolarizing voltages shows a 10 to 90% rise time of about 90 msec, and this is not very dependent on voltage (Fig. 8). A 10–90% rise time is used here because the time course of activation could not be fit by a single exponential, a feature which it has in common with most other delayed rectifiers, and because this measure of activation is independent of a kinetic model. The current also shows no evidence of inactivation in that there is no decay in the outward current with time even for depolarizing steps of tens of seconds in duration. Steady-state current voltage relationships determined with the cells held at a variety of holding potentials also show no dependence on the holding potential. A typical example of this is shown in Fig. 9 where cells bathed in a Ringer solution containing 40 mM external K were used to generate steady-state *I-V*'s from several holding potentials. The curves overlay within experimental error.

Blockers

Previous single-channel studies from these cells have shown that the large-conductance K channels were blocked by Ba and quinidine (Rae et al., 1990,

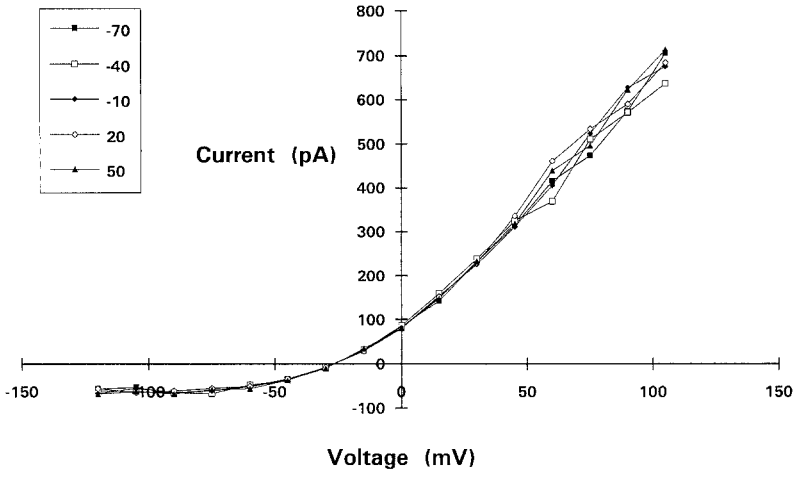

Fig. 9. An overplot of steady-state current-voltage relationships obtained from a cell bathed in 40 mM K/110 mM Na (Table). The cells were held at the transmembrane voltage shown in the inset before the voltage was stepped to the values shown on the x-axis. Upon completion of each step, the voltage was returned to the holding potentials specified in the inset. The curves show little or no sensitivity to holding potential.

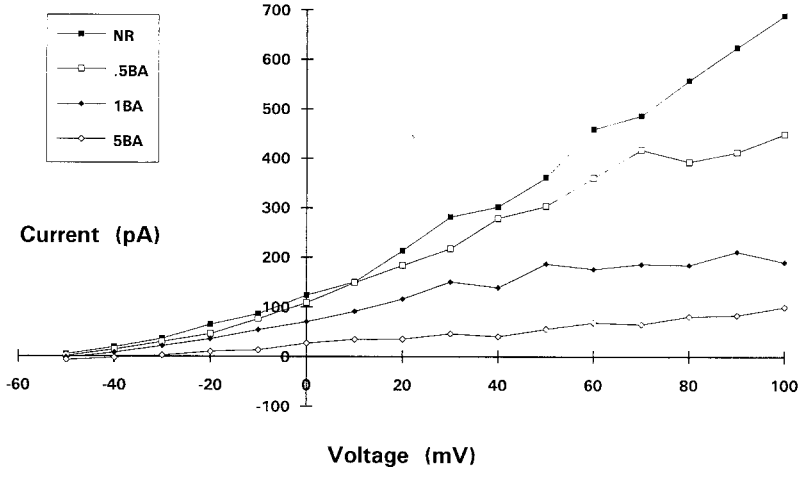

Fig. 10. Representative current-voltage relationships obtained from a single cell bathed in a normal Ringer solution containing the Ba concentrations shown in the inset. Both reduction of the steady-state current and shifts in the reversal potential are evident.

1992). We, therefore, tested the effect of these blockers on the whole-cell currents. A typical result of Ba blockade is shown in Fig. 10 where the steady-state current-voltage relationships from a cell bathed first in normal Ringer and then in normal Ringer containing several different Ba concentrations are overplotted. For the cell shown, the blockade increased as the Ba concentration was increased to 5 mM but even at this concentration, the blockade was not complete since the cell retained a resting voltage of about −35 mV. The Ba blockade was extremely variable from one cell to another. Most cells (6 of 10) showed the behavior depicted in Fig. 10, but in two cells, Ba neither shifted the reversal potential nor reduced the currents at any voltage. In two other cells, 5 mM Ba depolarized the cell to 0 mV and blocked the current quite completely. These results suggest that these cells contain two K conductances, one sensitive and one insensitive to Ba, and that the fractional representation of these currents varies from one cell to another. It was usually true that the Ba-insensitive current was small (0–100 pA) and so frequently could be ignored. Quinidine, on the other hand, at a concentration of 1 mM, always depolarized the cell to between −10 and 0 mV and blocked essentially everything but a leak current (Fig. 11). If there are two different K currents in this preparation as suggested by the Ba results, then quinidine must block them both.

Stimulation by Fenamates

Figure 12*A* shows current records from a cell held at −80 mV in normal Ringer which was then stepped to a series of depolarizing voltages in 10-mV steps. Figure 12*B* shows a similar set of currents except that the normal Ringer solution bathing the cell contained 500 μM flufenamic acid. Clearly, this particular fenamate remarkably increases the magnitude

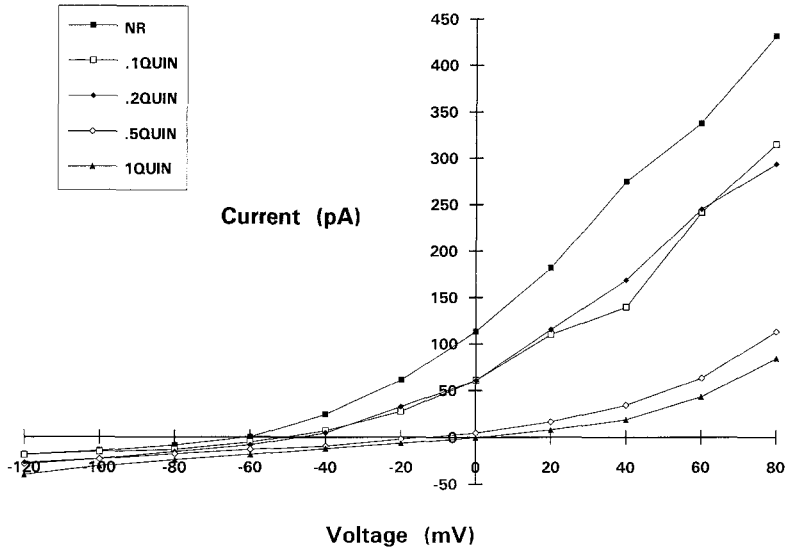

Fig. 11. Current-voltage relationships from a representative cell bathed in a normal Ringer solution containing the quinidine concentrations shown in the inset. Again, both reduction in the steady-state current and substantial shifts in the reversal potential are evident.

of the steady-state currents and also changes the apparent activation kinetics (25 of 29 cells). In the presence of flufenamic acid, the currents show little time-dependent activation; rather, the outward currents appear to be steps in response to step voltage changes. Similar results are obtained with mefenamic acid at 500 μM (26 of 28 cells) except that this fenamate has little effect on the activation time course. Comparable results were obtained with meclofenamic acid (2 of 2 cells) and niflumic acid (4 of 4 cells), other members of this family of compounds. In each instance, these compounds not only increased the size of the outward K currents, but also shifted the resting voltage of the cell in the direction of E_K. Even in cells that had no appreciable resting voltage in normal Ringer, voltages as negative as -50 mV could be obtained following the application of fenamates to the bathing solution. In cells with $\geqq -70$ mV resting voltages, the reversal potential shifts were, of course, less. In some cells, the reversal potential after fenamates was very close to -87 mV, E_K for these cells under the recording conditions. Figure 12*C* overplots the current-voltage relationships for a typical cell in normal Ringer, in Ringer with 500 μM flufenamic acid and for the difference current obtained by subtracting the family of currents generated in normal Ringer from those generated in normal Ringer plus 500 μM flufenamic acid. The difference current *I-V* demonstrates that the fenamate-dependent current is very highly K selective.

All four of the fenamates tested showed obvious effects over a 10–500 μM range and in fact produced near maximal responses by 500–1000 μM. The steady-state current increased monotonically as the concentration of the fenamates was increased, and the effect saturated by around 500–1000 μM. Full dose-response curves were determined at +90 mV for both mefenamic and flufenamic acid and are shown in Figs. 13*A* and *B*. In both cases, there is obvious stimulation of the current by 10 μM, and saturation occurs somewhere above 500 μM.

In an attempt to determine if the effect of the fenamates was to stimulate the existing current rather than activate a new current, we compared the blocker sensitivity of the fenamate-activated currents with that of the unstimulated current. Figure 14*A* and *B* overplots steady-state *I-V*'s of fenamate-stimulated currents in the presence and absence of the blockers Ba and diltiazem. Quinidine could not be tested because a precipitate formed when quinidine and any of the fenamates were mixed. Both the blockers used were effective in blocking the stimulated current. Diltiazem was much more effective in blocking the stimulated current than it was in blocking the resting current, a result that is easily explained by the fact that the open probability is higher in the presence of the fenamates. The detailed mechanism of diltiazem's action will have to be pursued with single-channel studies.

Fenamates Increase the Open Probability

Since the macroscopic current $I = niP_o$, an increase in the macroscopic current must involve either an increase in the number of channels (n), the single-channel conductance (i), or the probability that the channel is in the open state (P_o). It is unlikely that the number of channels is increased because the increase in the macroscopic current occurs within a second or two of the fenamate reaching the plasma

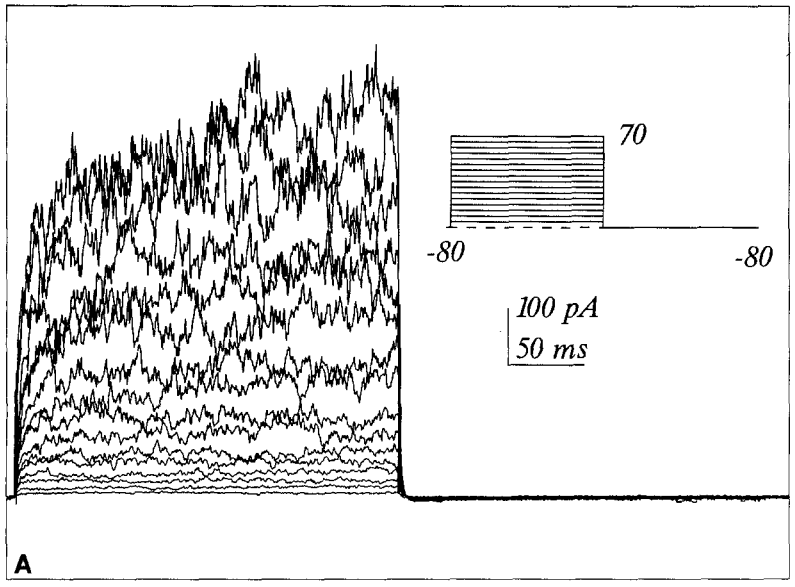

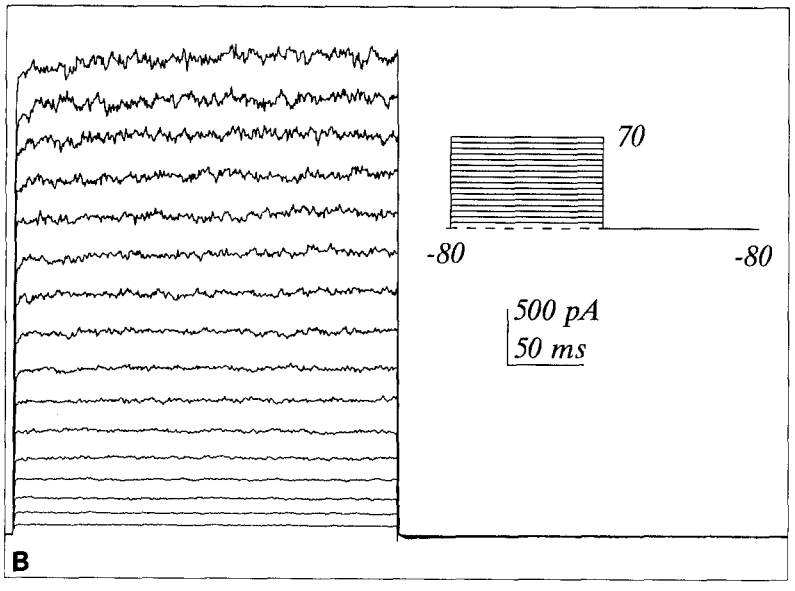

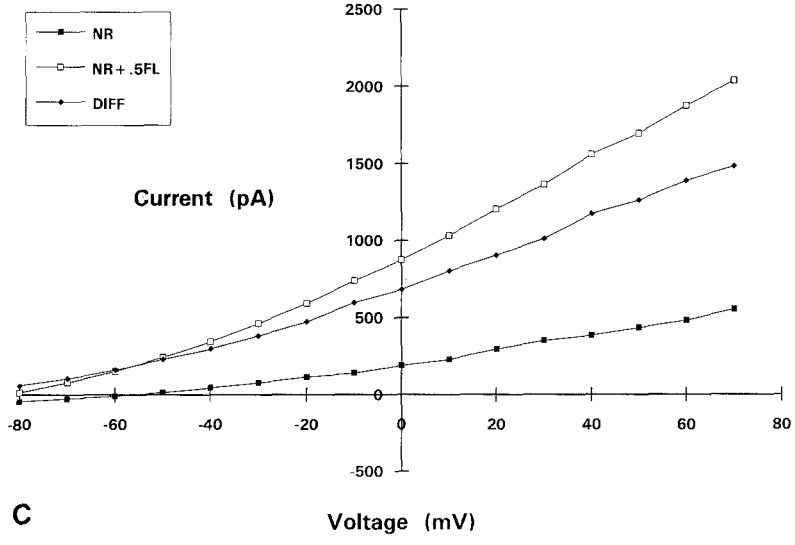

Fig. 12. Whole-cell current records from a single corneal epithelial cell bathed in (*A*) normal Ringer and (*B*) normal Ringer plus 500 μM flufenamic acid. (*C*) Steady-state current-voltage relationships obtained from *A* and *B* by subtracting *A* from *B* (*DIFF*). The fenamate-activated current is highly K selective, reversing clearly at some voltage more hyperpolarized than −80 mV (actual reversal *not shown*).

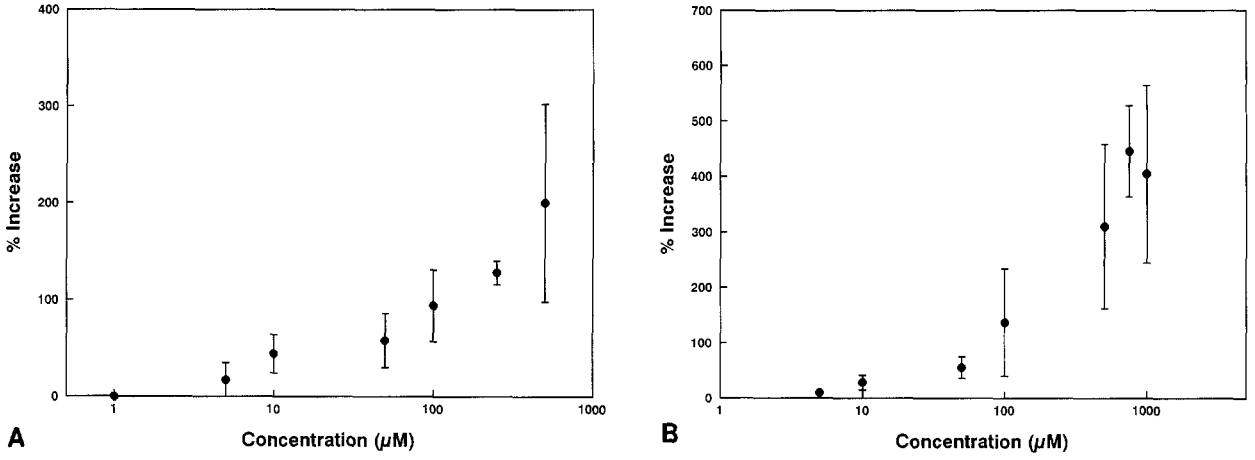

Fig. 13. Dose-response curves for the increase in current at 90 mV as a function of the external fenamate concentration (*A*) mefenamic acid and (*B*) flufenamic acid. Data is given as mean ± SD for $n = 5$.

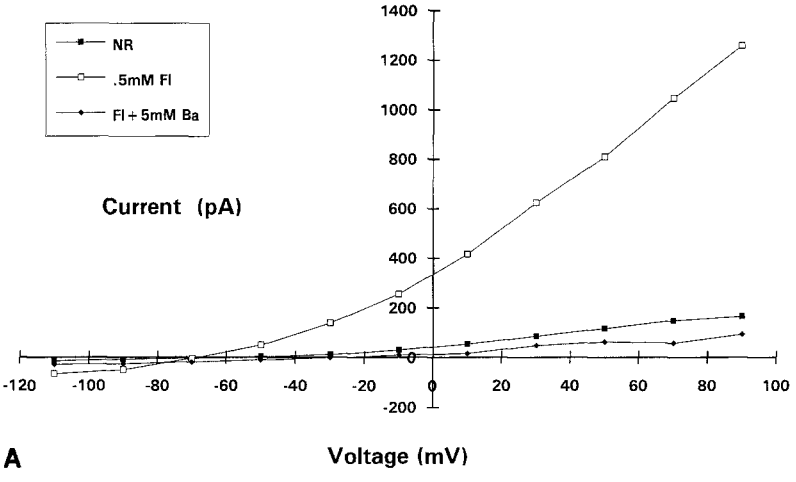

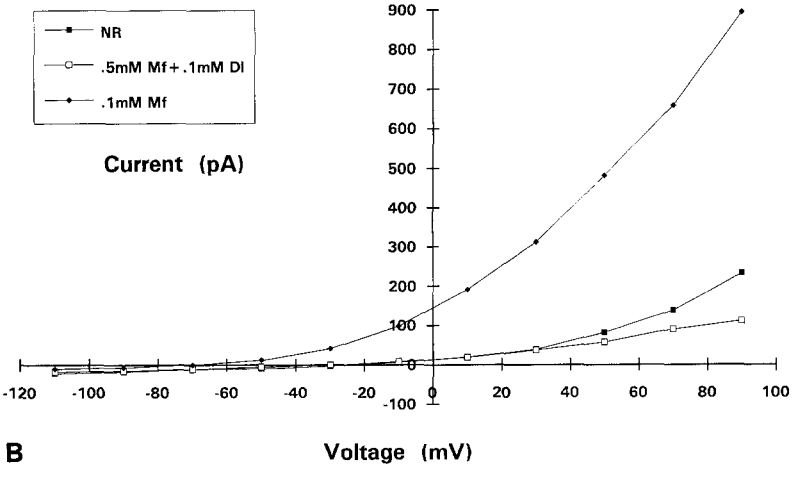

Fig. 14. Steady-state current-voltage relationships to show the effect of (*A*) 5 mM Ba and (*B*) 100 μM diltiazem on the flufenamic- and mefenamic-stimulated currents, respectively. Both blockers reduced the stimulated current down to a level comparable to that before the stimulation by fenamates occurred.

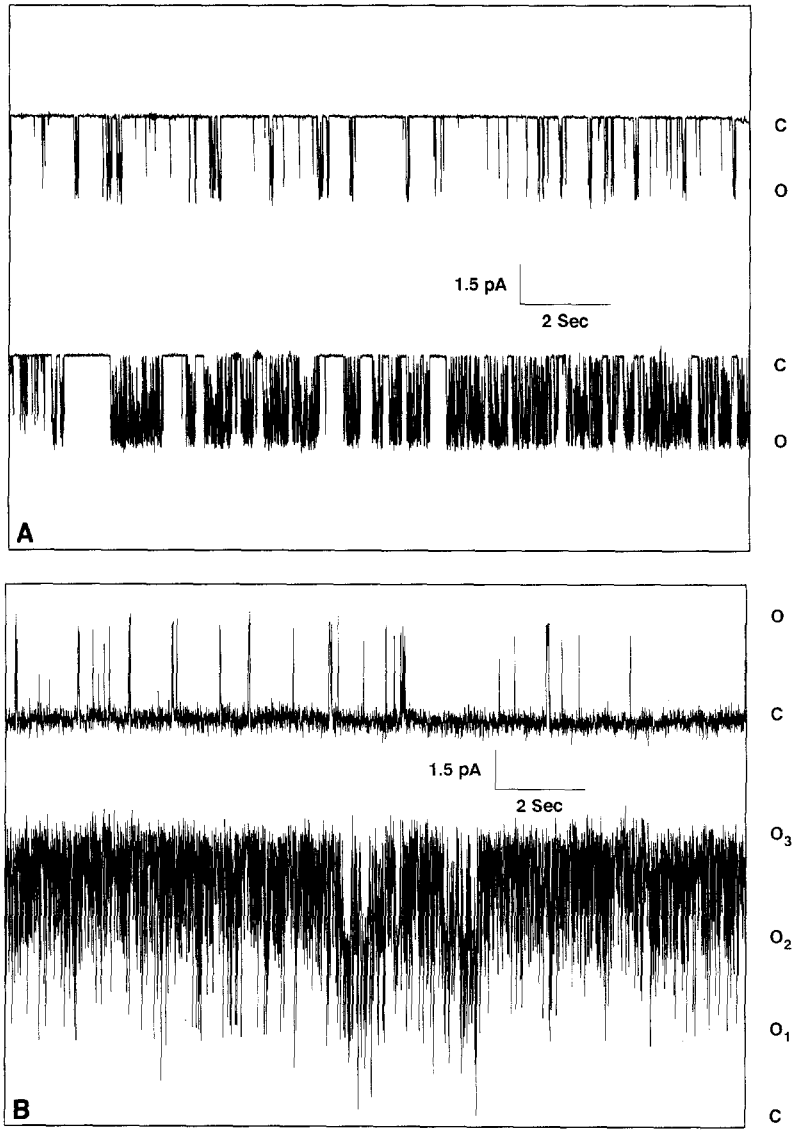

Fig. 15. Representative single-channel records showing the effect of (*A*) 500 μM mefenamic acid and (*B*) 500 μM flufenamic acid on single-channel currents. The records in *A* are from an inside-out patch where the mefenamic acid was applied to the normal Ringer bathing solution with 150 mM KCl Ringer in the pipette. The transmembrane potential was held at 0 mV. The records in *B* were obtained from a perforated outside-out vesicle where 500 μM flufenamic acid was added to the normal Ringer bathing solution with 150 mM KCl Ringer in the pipette at 0 mV transmembrane potential. In both *A* and *B*, the upper record is the control and the lower record is in the presence of the fenamate. The patch in *A* contained only one channel, whereas the preparation in *B* contained three. In both cases, the substantial activation by the fenamates is obvious.

membrane. This is certainly too fast for new channels to be synthesized and is probably too fast even for insertion of previously synthesized channels. We also did not see an increase in the number of channels in perforated outside-out vesicles following fenamate stimulation. We have no other independent data on this point. A change in the single-channel current also does not seem to be the mechanism by which fenamates act. Figure 15*A* and *B* show single-channel records before and after the application of mefenamic acid or flufenamic acid to the bath. While it is clear that the channels are open a much larger fraction of the time in the presence of mefenamic or flufenamic acids,there is no change in the size of the single-channel currents. These total results, therefore, make it likely that the major action of the fenamates is to increase the open probability.

An increase in open probability can also be demonstrated in the macroscopic currents. Figure 16*A* shows the results of a typical experiment in which the membrane was held at -80 mV, stepped to a series of 16 different depolarizing voltages and then returned to -80 mV at the end of each step. Again, by plotting the instantaneous tail current so generated against the voltage just prior to the -80-mV step which generated the tail currents, one obtains a curve that has the form of the open probability *versus* voltage curve for the channel. In this particular experiment, an elevated K solution was used in the bath so that the tail current would be large enough to measure easily. Since the K itself stimulates the open probability of the channel (*results not shown*), we overplot the tail currents in the elevated K solution with those from the elevated K solution

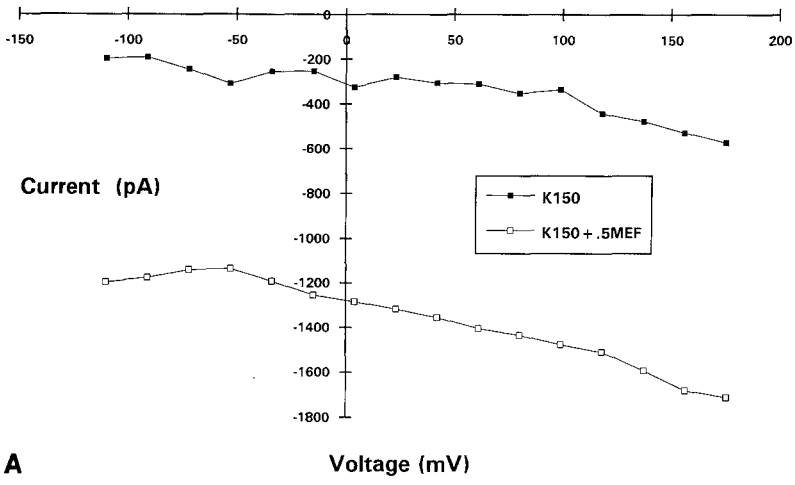

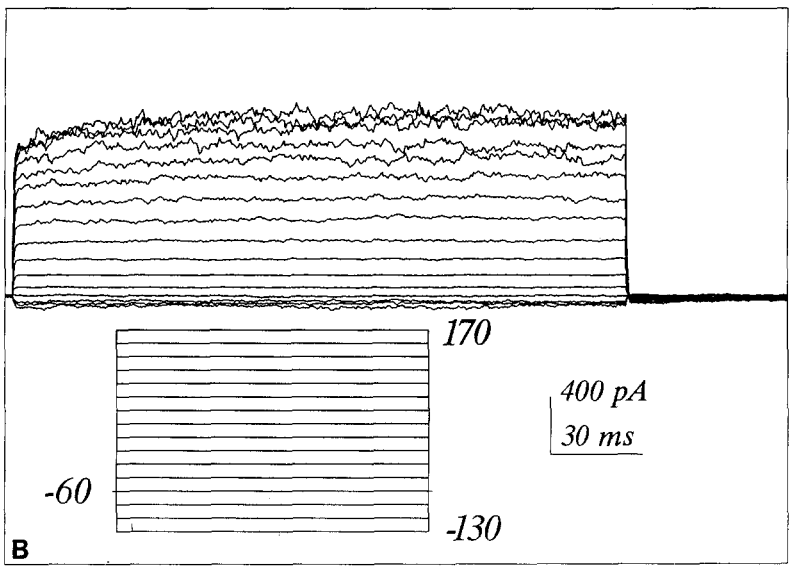

Fig. 16. (*A*) Overplot of tail currents obtained from a single cell bathed first in 150 mM K Ringer and then in the same Ringer solution containing 500 μM flufenamic acid. Note the lack of voltage dependence in that the ratio of tail currents at each voltage ≈ 4. Note also that the tail current in flufenamic acid begins to show some signs of saturation at about +170 mV. (*B*) Current records obtained in the presence of 150 mM K and 500 μM flufenamic acid. Note that the currents generated at +150 to +170 mV nearly overlay, showing saturation of the outward current.

plus fenamate. These results show clearly that the tail current increases by about four times at all voltages in the presence of flufenamic acid but still does not quite reach a plateau even by 170 mV. A plateau in the current could occur when the open probability is near unity. Figure 16*B* presents current records obtained in the presence of K and flufenamic acid. These records show that in some cells, the outward currents and the respective tail currents (*data not shown*) can become saturated at voltages exceeding 150 mV. The results presented make it certain that an increase in open probability accompanies fenamate addition, but none of our whole-cell experiments completely exclude the possibility that the number of channels also increases.

Is the Fenamate Effect Directly on the Channel?

To determine if the action of fenamates was directly on the channel or via some indirect mechanism, we did a variety of single-channel experiments. In the first, the pipette tip was filled with a Ringer solution lacking the fenamates and the remainder of the electrode backfilled with the same solution containing the fenamates. The electrode was used to obtain a gigohm seal to the cell, and channel activity was recorded. In some instances, initially no channel activity was occurring spontaneously but since the channels can be activated by suction in the pipette, it was possible to verify the existence of the channels in the patch without natural gating occurring. In every instance, following a diffusion delay, the channels became activated to a higher open probability in a time period expected for the diffusion of the fenamates to the membrane patch. These experiments demonstrated the action of the fenamates when applied exclusively to the membrane patch. In a second set of experiments, the pipette was filled with a normal Ringer solution completely lacking fenamates and then gigohm sealed to the cell. Following verification of the existence of channels in

the patch, the fenamates were added to the bathing solution surrounding the individual cells. Both mefenamic acid and flufenamic acid stimulated the channel currents when applied to the bath. They again did so within a few seconds of the fenamate contacting the plasma membrane. These results might normally be taken as evidence for the role of a second messenger. In a third series of experiments, the electrodes were filled with a fenamate-lacking Ringer solution, gigohm sealed to the cell and channel existence verified. Then the patch was excised into an inside-out configuration. In each case, it was verified that no vesicle had formed. Addition of either mefenamic acid or flufenamic acid to the bath and thus to the interior surface of the inside-out patch, also activated the currents.

Discussion

The largest current that flows in the dissociated rabbit cornea epithelium at rest or at any of the depolarizing voltages studied comes primarily from the large-conductance K channels which have been described previously in this tissue (Rae et al., 1990). In this study, it was possible to show, at least at strongly depolarizing voltages, that the whole-cell currents were contributed by single channels having a conductance between 160 and 170 pS with physiological levels of internal K. It was not possible to measure these currents unambiguously at voltages where the single-channel currents were small, and so from this criterion alone, one cannot exclude the existence of other channels in this preparation. In fact, in many cells it was possible to demonstrate quite conclusively that two different K currents existed. The first was presumably due to these large-conductance channels and was blocked nearly completely by 5 mM Ba in the external solution. In several cells, complete blockade of these channels did not cause the cell resting voltage to go to 0 mV and in fact in those cases, the resting voltage could be as negative as −40 mV. This result is most likely due to a K-selective current in parallel with a leak conductance which remained in the cell following Ba blockade. In these same cells, it was possible to use 1 mM quinidine which proved in almost every instance to block virtually all of the current except the leak and to cause the cell resting voltage to go to near 0 mV. In a few cells where the current was particularly small, Ba had no effect, whereas quinidine at 1 mM completely blocked the current. In these cells, we presume that only the second K conductance existed. To date, we have not been successful in identifying the single channels that are responsible for the small current but have reason to believe from studies on outside-out perforated vesicles that either the single-channel conductance is below the resolution of our patch-clamp measurements or that the current comes from some sort of electrogenic transporter that is not a channel. We are unable to decide between the two with existing data.

The major K current which we recorded is active at the resting voltage of the cell (around −60 mV) and so is a likely candidate for control of the resting voltage. We show here that the channel is active even at voltages more negative than −100 mV and that the open probability begins to show obvious increase at about −100 mV for cells bathed in normal Ringer. The probability of channel opening is very weakly voltage dependent, increasing monotonically as the transmembrane voltage is depolarized. In cells bathed in normal Ringer solution or in 20 to 40 mM external K, the instantaneous tail currents following activating voltages to as high as +200 mV were still increasing in size. This suggests that the open probability had not yet reached unity even by +200 mV. We show that external fenamates can quickly increase the K current by as much as four- to fivefold. If one presumes that this happens too rapidly for new channels to have been inserted in the membrane, then an increase in the open probability is the likely result of the action of these compounds. This result is strengthened by the fact that for cells held at −80 mV, the instantaneous current generated by depolarizing voltage steps is increased in the presence of fenamates. This is expected if the open probability at −80 mV is increased by the fenamates. Tail currents generated in the presence of fenamates also show a four- to fivefold increase in amplitude at all voltages. Therefore, a simple shift in the voltage dependence of open probability is not the mechanism of action. If fenamates can increase the current by four- to fivefold at 100 mV in the absence of an increase in the number of channels or an increase of single-channel current (*see* Figs. 16*B* and *C*), then the open probability in the absence of fenamates could not exceed about 0.2 at +100 mV. A channel which opens at −100 mV and reaches 0.2 open probability at +100 mV is certainly not very dependent on voltage for its activation. The channel also does not show voltage dependence in its opening kinetics. The 10–90% rise time of its activation is about 90 msec and essentially independent of voltage.

The currents that we measure here are not quite the same as those suggested from recent macroscopic studies by Wolosin and Candia (1987*b*). In their studies on both bullfrog and rabbit corneas, they postulated the existence of two K currents. One was a resting current that was blocked by Ba but not quinidine, and the other was a volume-activated current blocked by both Ba and quinidine. Of the

two currents that we report, the small background current is insensitive to Ba, whereas both currents are nearly completely blocked by quinidine. It is reasonable to suspect that our stretch-activated channel could be involved in volume regulation, and that possibility is presently under investigation. Reinach (1985) also showed that the K conductance in corneal epithelium in bullfrog could be blocked by both Ba and diltiazem. We find that our large-conductance channel is blocked also by Ba and diltiazem but that the block by diltiazem is very small when the channel has a low open probability like we find at rest. Clearly, additional work will be required before our single-channel and whole-cell currents can be rationalized with these previous more macroscopic experiments.

We are grateful to Erika Wohlfiel for secretarial help, Helen Hendrickson for cell preparation, and Joan Rae for software development. This work was supported by NIH grants EY06005 and EY03282 and an unrestricted award from Research to Prevent Blindness.

References

Akaike, N. 1971. The origin of the basal cell potential in frog corneal epithelium. *J. Physiol.* **219:**57–75

Akaike, N., Hori, M. 1970. Effect of anions and cations on membrane potential of rabbit corneal epithelium. *Am. J. Physiol.* **219:**1811–1818

Candia, O.A., Cook, P. 1986. Na^+-K^+ pump stoichiometry and basolateral membrane permeability of frog corneal epithelium. *Am. J. Physiol.* **250:**F850–F859

Candia, O.A., Grillone, L.R., Chu, T.-C. 1986. Forskolin effects on frog and rabbit corneal epithelium ion transport. *Am. J. Physiol.* **251:**C448–C454

Candia, O.A., Schoen, H.F. 1978. Selective effects of bumetanide on chloride transport in bullfrog cornea. *Am. J. Physiol.* **234:**F297–F301

Clausen, C., Reinach, P.S., Marcus, D.C. 1986. Membrane transport parameters in frog corneal epithelium measured using impedance analysis techniques. *J. Membrane Biol.* **91:**213–225

Ehlers, N. 1970. Intracellular potentials of the corneal epithelium. *Acta Physiol. Scand.* **78:**471–477

Fee, J.P., Edelhauser, H.F. 1970. Intracellular electrical potentials in the rabbit corneal epithelium. *Exp. Eye Res.* **9:**233–240

Gogelein, H., Dahlem, D., Englert, H.C., Lang, H.J. 1990. Flufenamic acid, mefenamic acid and niflumic acid inhibit single nonselective cation channels in the rat exocrine pancreas. *FEBS Lett.* **268:**79–82

Gogelein, H., Pfannmuller, B. 1989. The nonselective cation channel in the basolateral membrane of rat exocrine pancreas. *Pfluegers Arch.* **413:**287–298

Huff, J.W., Reinach, P.S. 1985. Mechanism of inhibition of net ion transport across frog corneal epithelium by calcium channel antagonists. *J. Membrane Biol.* **85:**215–223

Keys, C., Nelson, S., Deutsch, W., Rae, J. 1986. Patch clamp recordings from mammalian corneal epithelium. *Invest. Ophthalmol. Vis. Sci.* **27:**350*a*

Klyce, S.D. 1972. Electrical profiles in the corneal epithelium. *J. Physiol.* **226:**407–429

Klyce, S.D. 1973. Relationship of epithelial membrane potentials to corneal potential. *Exp. Eye Res.* **15:**567–575

Klyce, S.D. 1975. Transport of Na, Cl, and water by the rabbit corneal epithelium at resting potential. *Am. J. Physiol.* **228:**1446–1452

Klyce, S.D., Crosson, C.E. 1985. Transport processes across the rabbit corneal epithelium: A review. *Curr. Eye Res.* **4:**323–331

Knauf, P.A., Mann, N.A. 1984. Use of niflumic acid to determine the nature of the asymmetry of the human erythrocyte anion exchange system. *J. Gen. Physiol.* **83:**703–725

Lewis, G.N., Sargent, L.W. 1909. Potentials between liquids. *J. Am. Chem. Soc.* **31:**363–367

Marshall, W.S., Hanrahan, J.W. 1991. Anion channels in the apical membrane of mammalian corneal epithelium primary cultures. *Invest. Ophthalmol. Vis. Sci.* **32:**1562–1568

Marshall, W.S., Klyce, S.D. 1984. Cellular mode of serotonin action on Cl^- transport in the rabbit corneal epithelium. *Biochim. Biophys. Acta* **778:**139–143

Nagel, W., Carrasquer, G. 1989. Effect of loop diuretics on bullfrog cornea epithelium. *Am. J. Physiol.* **256:**C750–C755

Rae, J.L., Dewey, J., Rae, J.S. 1992. The large conductance potassium channel of rabbit corneal epithelium is blocked by quinidine. *Invest. Ophthalmol. Vis. Sci.* **33:**286–290

Rae, J.L., Dewey, J., Rae, J.S., Nesler, M., Cooper, K. 1990. Single potassium channels in corneal epithelium. *Invest. Ophthalmol. Vis. Sci.* **31:**1799–1809

Rae, J.L., Levis, R.A., Eisenberg, R.S. 1988. Ionic channels in ocular epithelia. *In:* Ion Channels. T. Narahashi, editor. pp. 283–327. Plenum, New York

Reinach, P.S. 1985. Roles of cyclic AMP and Ca in epithelial ion transport across corneal epithelium: A review. *Curr. Eye Res.* **4:**385–391

Reinach, P.S., Candia, O.A., Alvarez, L.J. 1979. Energetic requirements of active transepithelial Na and Cl transport in the isolated bullfrog cornea. *Exp. Eye Res.* **29:**637–646

Reinach, P., Nagel, W. 1984. Basolateral membrane K conductance of frog corneal epithelium. *Fed. Proc.* **43:**893*a*

Reinach, P., Nagel, W. 1985. Implications of an anomalous intracellular electrical response in bullfrog corneal epithelium. *J. Membrane Biol.* **87:**201–209

Reinach, P.S., Schoen, H.F. 1990. NPPB inhibits the basolateral membrane K^+ conductance in the isolated bullfrog cornea. *Biochim. Biophys. Acta* **1026:**13–20

Reinach, P.S., Thurman, C., Klemperer, G. 1987. Basolateral membrane K permselectivity and regulation in bullfrog cornea epithelium. *J. Membrane Biol.* **99:**205–213

Reuss, L., Reinach, P., Weinman, S.A., Grady, T.P. 1983. Intracellular ion activities and Cl^- transport mechanisms in bullfrog corneal epithelium. *Am. J. Physiol.* **244:**C336–C347

Terada, H., Muraoka, S., Fujita, T. 1974. Structure-activity relationships of fenamic acids. *J. Med. Chem.* **17:**330–334

Wangemann, P., Wittner, M., Di Stefano, A., Englert, H.C., Lang, H.J., Schlatter, E., Greger, R. 1986. Cl^--channel blockers in the thick ascending limb of the loop of Henle. Structure activity relationship. *Pfluegers Arch.* **407:**S128–S141

White, M.M., Aylwin, M. 1990. Niflumic and flufenamic acids are potent reversible blockers of Ca^{2+}-activated Cl^- channels in *Xenopus* oocytes. *Mol. Pharmacol.* **37:**720-724

Wiederholt, M., Koch, M. 1978. Intracellular potentials of isolated rabbit and human corneal epithelium. *Exp. Eye Res.* **26:**629–640

Wolosin, J.M. 1988. Regeneration of resistance and ion transport in rabbit corneal epithelium after induced surface cell exfoliation. *J. Membrane Biol.* **104:**45–55

Wolosin, J.M., Candia, O.A. 1987*a*. Cl^- secretagogues increase basolateral K^+ conductance of frog corneal epithelium. *Am. J. Physiol.* **253:**C555–C560

Wolosin, J.M., Candia, O.A. 1987*b*. Volume regulatory decrease in corneal epithelium. *Ann. NY Acad. Sci.* **494:**296–298

Received 8 November 1991; revised 5 March 1992